

## On the Physical Parameters and Relaxation Processes in Nematic Azobenzene Polymers for Optical Nanowriting

Laura Andreozzi,<sup>\*1</sup> Massimo Faetti,<sup>1</sup> Giancarlo Galli,<sup>2</sup> Marco Giordano,<sup>1</sup> Diego Palazzuoli<sup>1</sup>

<sup>1</sup>INFM Unit of Pisa and Department of Physics, University of Pisa, Italy

<sup>2</sup>Department of Chemistry and Industrial Chemistry, University of Pisa, Italy

**Summary:** The possibility of achieving devices for rewritable optical storage is provided by liquid-crystalline polymers with azobenzene side groups, because they undergo photochemically induced *trans-cis* reversible isomerization. In this work we overview our investigations into a nematic azobenzene-polymethacrylate (PMA4) as a suitable material for optical nanowriting. Relaxation processes over different time-length scales are discussed with particular reference to understanding the interplay between homogeneity at the molecular level, bit stability and working temperature range.

**Keywords:** azobenzene; ESR; liquid-crystalline polymers (LCP); nanowriting; nematic; optical storage; relaxation

### Introduction

Investigations into optical writing on polymeric substrates are in a state of flux. In the last years side group liquid-crystalline polymers have largely been investigated due to their potential application as media for optical information storage.<sup>[1]</sup> In particular, nematic polymethacrylates (PMA4) containing a 3-methyl-4'-pentyloxy-azobenzene mesogenic unit connected at the 4-position by a hexamethylene spacer to the polymer main chain have proved to be useful candidate materials for such applications.<sup>[2-9]</sup>

The basic process of optical writing in azobenzene polymers is the photoisomerization of the azobenzene unit. UV radiation excites the *trans-cis* transition, while blue radiation produces *trans-cis-trans* cycle leading to the reorientation of the azobenzene electric dipole. The presence of the *cis* isomer frustrates the nematic phase, and a cooperative rearrangement of the polymer chain takes place. Therefore, birefringence and/or topographic relief can be induced locally depending on the optical irradiation. The ultimate size of the obtainable optically induced bit is not yet determined. A guess of such dimension is on the order of the cooperativity or entanglement lengths (~3 nm or ~10 nm, respectively).<sup>[10]</sup> In terms of data storage density that would correspond to about 1 Tbit/cm<sup>2</sup>.

Optical writing from mm to nm length scales and relaxation processes at different length and time scales in PMA4 have been investigated.<sup>[2-9]</sup> Crucial parameters in data storage were found to be bit stability, homogeneity at molecular level, and working temperature range.<sup>[1,2-4]</sup> Homogeneity of the polymeric matrix strongly depends on the thermal procedure.<sup>[3,4]</sup> On the other hand, various relaxation processes can affect the bit stability even if backbone conformational rearrangements can stabilize stored information over a larger temperature range. Therefore, in our work we used experimental techniques covering different time and length scales in order to fully characterize the nematic matrices of interest (PMA4).

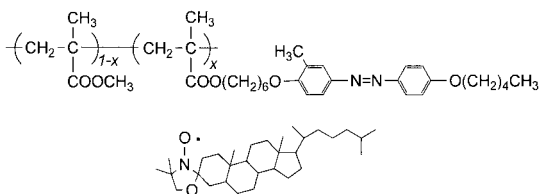


Figure 1. Structures of the azobenzene homopolymer ( $x = 1$ ) and copolymer 30/70 ( $x = 0.7$ ) host matrices (PMA4) and the cholestane spin probe guest.

## Materials and Experimental

Two homopolymer samples (S1 and S5) and a 30/70 copolymer sample ( $x = 0.7$ ) (Table 1) were prepared by free-radical polymerization according to a literature procedure (Figure 1).<sup>[11]</sup> Average molar masses were determined by size exclusion chromatography (SEC) of chloroform solutions using polystyrene standard samples for calibration.

Table 1. Physico-chemical characteristics of the polymer samples.

Sample	$M_w$ (g/mol)	$M_w/M_n$	$T_g$ (K)	$T_c$ (K)	$T_{NI}$ (K)
Homopolymer (S1)	59,000	3.17	294	320	353
Homopolymer (S5)	72,500	2.43	305	337	357
30/70 Copolymer	117,000	3.54	314	----	345

Differential scanning calorimetry (DSC) measurements were performed with a Perkin-Elmer DSC7 calorimeter calibrated with indium. Along with the  $T_g$  and the nematic-isotropic temperature,  $T_{NI}$ , the DSC traces (10 K/min heating rate) also evidenced a particular step associated to a conformational transition at the temperature  $T_c$ .<sup>[15]</sup>

Rheological measurements in oscillatory regime were carried out with a Haake Rheostress RS150H rheometer in the plate-cone geometry in the temperature range 400–324 K. The temperature dependences of the structural relaxation time in the investigated regions were well described by the Vogel-Fulcher (VF) law with parameters  $T_0 = 259 \pm 5$  K and  $T_b = 1300 \pm 50$  K for the homopolymer and  $T_0 = 266 \pm 5$  K and  $T_b = 1570 \pm 50$  K for the copolymer.

ESR studies were performed on the polymeric matrices in which the cholestane molecular tracer was dissolved ( $10^{-3}$  cholestane/repeat unit mole ratio) (Figure 1). An X band Bruker ER 200 SRL was used and the temperature control ( $\pm 0.1$  K accuracy) was ensured by a Bruker BVT100 system. In order to study the temperature dependence of the probe dynamics on thermal treatment, a special protocol was followed as is detailed elsewhere.<sup>[3,4]</sup>

ESR spectra were simulated by using a theoretical approach based on generalized Mori theory.<sup>[12]</sup> The cholestane spin probe exhibits nearly axial symmetry.<sup>[13]</sup> Its reorientational dynamics in the present polymer matrices was characterized by a spinning motion around its own symmetry axis and a tumbling motion of the symmetry axis itself with correlation times  $\tau_{\parallel}$  and  $\tau_{\perp}$ , respectively. The anisotropy ratio  $\tau_{\perp}/\tau_{\parallel}$  was found to be 15 for the homopolymer and 18 for the copolymer over the whole temperature range. Therefore, only the temperature dependence of  $\tau_{\parallel}$  will be shown. The greater anisotropy ratio found in the copolymer denoted that the reorientation of the molecular tracer occurred in a more rigid molecular environment. The principal components of the magnetic tensors of the spin probe were drawn by the powder line-shapes<sup>[14]</sup> of the linear ESR recorded at 143 K, according to the procedure described elsewhere.<sup>[15]</sup> Powder line-shapes in the polymer samples were found to be coincident; the values of the Zeeman and hyperfine tensors in the molecular frame are listed in Table 2.

For optical experiments on the mm length scale, the samples were prepared by solution casting yielding reasonably homogeneous specimens of about 10  $\mu\text{m}$  thickness. The optical observations were carried out with a Zeiss Axioplan 2 polarizing microscope connected to a video camera for recording of the images. The sample was placed between crossed polarizers and an interferometric filter (wavelength center  $\lambda = 650.2$  nm, bandwidth  $\Delta\lambda = 91$  nm) was used to monitor the system without inducing any isomerization cycle. To obtain a small optical spot, the field diaphragm aperture was reduced to the minimum size and the optical

filter was removed. The results of experiments performed on  $\mu\text{m}$  and  $\text{nm}$  length scales are also reported here.<sup>[2,9]</sup>

Table 2. Values of the principal components of the Zeeman and hyperfine tensors in the molecular reference frame for cholestane.

$g$			$A$ (gauss)		
$g_{xx}$	$g_{yy}$	$g_{zz}$	$A_{xx}$	$A_{yy}$	$A_{zz}$
2.0026	2.0092	2.0069	32.6	5.5	5.0

## Results and Discussion

Many efforts were made to carefully take into account the inhomogeneous nature of the ESR experimental line-shape.<sup>[16]</sup> The analysis led us to recognize the bimodal character of the distribution function of the spin-probe sites. In fact, a two- $\delta$  distribution function of the correlation times with fast and slow reorienting sites was shown to reproduce the experimental line-shape better than log-Gauss and square distributions. Moreover, we proved that assuming a bimodal log-Gauss distribution did not improve the result obtained with the two- $\delta$  distribution.<sup>[16]</sup> The temperature dependences of the spinning correlation times of both fast and slow components for sample S1 after annealing at  $T_a = 383$  K or 358 K are reported in Figure 2. The non-Arrhenius behaviors are well reproduced by the VF law:

$$\tau_{\parallel} = \tau_{\parallel 0} \exp[T_b/(T - T_0)] \quad (1)$$

in which  $\tau_{\parallel 0}$  and  $T_b$  are constants which depend on the polymer and the spin probe. The values of the parameters for the different temperature branches of both slow and fast dynamics are summarized in Table 3. Note that the VF temperature values coincide with those obtained by rheological measurements. Therefore, the spinning correlation time behavior could be expressed by a fractionary law of the structural relaxation time  $\tau_{\alpha}$ :

$$\tau_{\parallel} \propto \tau_{\alpha}(T)^{\xi} \quad (2)$$

in which  $\xi$ , the fractional exponent, may vary between 0 and 1, with  $\xi = 1$  corresponding to a complete coupling of the probe dynamics to the structural relaxation of the host matrix.

Starting from studies of spin probe dynamics dissolved in molecular glass-formers,<sup>[3]</sup> the fractionary coefficient relevant to the probe dynamics at higher temperatures was traced to steric hindrance due to specific local characteristic of the host matrix, meanwhile the one

relevant to lower temperatures was ascribed to the onset of cooperativity in the dynamics.<sup>[3]</sup> Moreover, the analysis of the decoupling degree of probe dynamics from structural relaxation allowed to evidence the space character of the heterogeneities detected in the host matrices.<sup>[16]</sup>

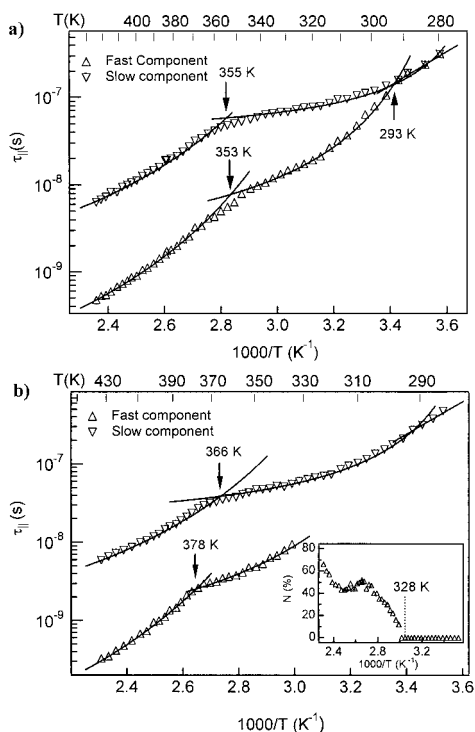


Figure 2. Temperature dependence of ESR correlation times in PMA4 (S1) for the annealing procedure at  $T_a = 383$  K (a) or  $358$  K (b). The inset shows the population ( $N$ ) of the fast component.

The crossover to the Arrhenius regime, when present, occurred in the proximity of the glass transition. It is apparent that very different dynamic behaviors characterize the probe molecular rotation in differently annealed polymeric matrix. The presence of the fast and the slow molecular sites in the whole temperature range denotes the greatly heterogeneous character of the polymeric matrix annealed at  $383$  K (Figure 2a). By contrast, the fast component was unstable in the polymeric host matrix after annealing at  $358$  K.

Table 3. Fit parameters of the VF law for the fast and slow components in different temperature regions after annealing homopolymer S1 at 383 K or 358 K.

Temperature range	$\tau_{l_0}$ (s)	$T_0$ (K)	$T_b$ (K)
$T_a = 383$ K			
H.T. (F)	$(1.2 \pm 0.1) \cdot 10^{-11}$	$259 \pm 3$	$608 \pm 27$
L.T. (F)	$(1.4 \pm 0.1) \cdot 10^{-9}$	$258 \pm 8$	$164 \pm 9$
H.T. (S)	$(3.3 \pm 0.3) \cdot 10^{-10}$	$259 \pm 3$	$497 \pm 4$
L.T.(S)	$(3.6 \pm 0.3) \cdot 10^{-8}$	$259 \pm 4$	$47 \pm 2$
$T_a = 358$ K			
H.T. (F)	$(3.3 \pm 0.2) \cdot 10^{-12}$	$258 \pm 9$	$799 \pm 60$
L.T.(F)	$(3.0 \pm 0.2) \cdot 10^{-10}$	$258 \pm 7$	$258 \pm 15$
H.T. (S)	$(3.0 \pm 0.2) \cdot 10^{-10}$	$258 \pm 7$	$527 \pm 20$
L.T.(S)	$(1.6 \pm 0.1) \cdot 10^{-8}$	$258 \pm 8$	$97 \pm 7$

In fact it disappeared at about 328 K, that is very close to the conformational transition temperature  $T_c$  (Table 1). Thus, thermal annealing treatments slightly above  $T_{NI}$  are preferable in order to obtain a homogeneous matrix suitable for optical writing.<sup>[2]</sup>

In Figure 3 the temperature dependences of the spinning correlation times of both fast and slow components for copolymer 30/70 and homopolymer S1 after annealing at  $T_a = 358$  K are reported. The values of the physical parameters characterizing the different dynamic regimes are reported in Table 4. Once again it should be noted that the thermal treatment at 358 K provides a homogeneous substrate; the fast component appears to be quite unstable and disappears at about 358 K. This finding suggests that an optically induced bit in the copolymer could be stable well above the glass transition temperature at higher temperatures than in the corresponding homopolymer.

In order to test the effectiveness of polymer conformation on optical bit stability, optical experiments were performed. Figure 4 shows the optical writing, at the mm scale, obtained in different originally isotropic samples. It is apparent how the temperature range of stability could be extended by selecting polymers with a higher molar mass, compare S5 ( $M_w = 72500$  g/mol) to S1 ( $M_w = 59000$  g/mol).

Table 4. Fit parameters of the VF law for the fast and slow components in different temperature regions after annealing copolymer 30/70 at 358 K.

Temperature range	$\tau_{l_0}$ (s)	$T_0$ (K)	$T_b$ (K)
H.T. (F)	$(2.9 \pm 0.2) \cdot 10^{-12}$	$266 \pm 7$	$820 \pm 70$
H.T. (S)	$(2.0 \pm 0.1) \cdot 10^{-9}$	$266 \pm 6$	$290 \pm 20$
L.T. (S)	$(2.2 \pm 0.1) \cdot 10^{-8}$	$266 \pm 8$	$94 \pm 6$

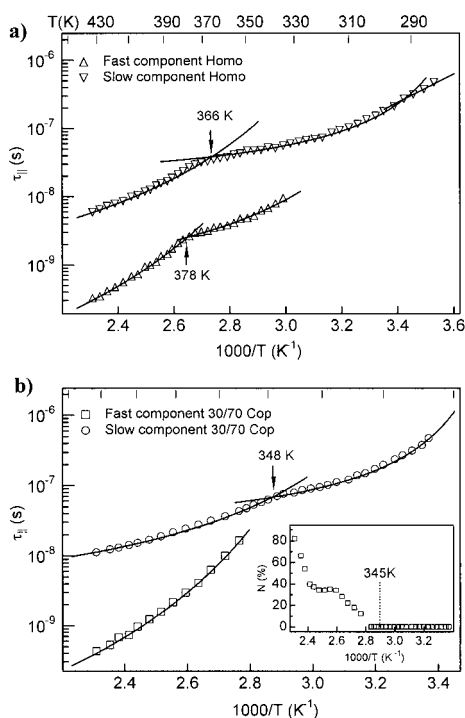


Figure 3. Temperature dependence of ESR correlation times in PMA4 homopolymer S1 (a) and 30/70 copolymer (b) for the annealing procedure at  $T_a = 358$  K. The inset shows the population ( $N$ ) of the fast component.

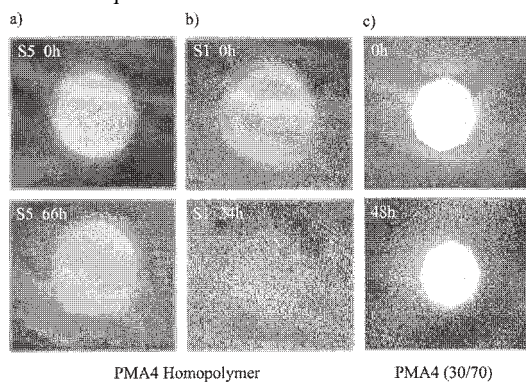


Figure 4. Optical writing performed at 338 K by white light irradiation at the polarizing microscope: homopolymers S5 (a) and S1 (b), and 30/70 copolymer (c).<sup>[5,6]</sup>

This results from spontaneous conformational rearrangements that occur at higher temperatures in the polymer with greater molar mass.<sup>[5]</sup> The same thermal procedure and writing experiments were performed on the PMA4 copolymer.<sup>[6]</sup> No appreciable decrease of birefringence was detected (Figure 4c), and the optically induced bit remained stable during 48 h monitoring. It can be envisaged that the main chain conformation modified by the optically induced orientation of the side chains was stabilized by the methyl methacrylate counits in the copolymer.

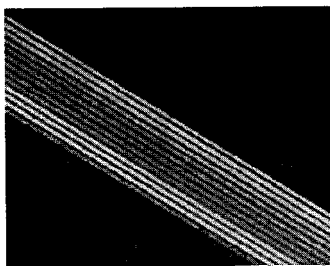


Figure 5. Polarizing optical microscopy image ( $1000 \times 850 \mu\text{m}^2$ ) of lines written by polarized light on a PMA4 S1 film, at varying fluence ( $0.65\text{--}3.15 \text{ J/cm}^2$ ).<sup>[2]</sup>

Experiments carried out at the  $\mu\text{m}$  length scale<sup>[2]</sup> (Figure 5) provided an estimate of the optical writing rate on  $10 \mu\text{m}$  thick films of S1. The time necessary to induce a  $5 \times 5 \mu\text{m}^2$  dot in birefringence was evaluated to be of about 0.5 ms.

Scanning near-field optical microscopy (SNOM) allowed to push the bit size down to the range of 50–100 nm.<sup>[7,9]</sup> The aperture of the SNOM optical sensors was used as the localized light source for the writing process, as well as for detecting the anisotropic optical properties of the sample, by adopting a polarization-modulation technique sensitive to local dichroism, on the sub-wavelength scale.<sup>[17]</sup> The sample topography was simultaneously recorded with nanometer resolution. Typical apertures of 50 to 150 nm are commercially available. PMA4 films of around 100 nm thickness were spin coated onto quartz slides.

Figure 6 shows examples of nanostructures created by SNOM with 325 nm laser light that exclusively enables the *trans-cis* isomerization, thus eventually deforming the surface. The topographic structures were obtained at room temperature and have 180, 75 and 45 nm width, respectively. The intrinsic limit of aperture probes ( $\sim 50 \text{ nm}$ ) was thus reached. All-optical



writing/reading was achieved by using red light at the SNOM sensor to probe the optical properties without destroying the written bits.

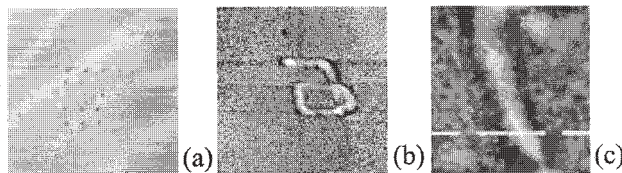


Figure 6. SNOM topography images of the optically nanostructured PMA4 thin film of (a) homopolymer S1 (exposure time = 1 s/dot, image size =  $5 \times 5 \mu\text{m}^2$ ), (b) 30/70 copolymer (speed = 20 nm/s, size =  $2 \times 2 \mu\text{m}^2$ ) and (c) 30/70 copolymer (speed = 50 nm/s, size =  $300 \times 300 \text{ nm}^2$ ).<sup>[7,9]</sup>

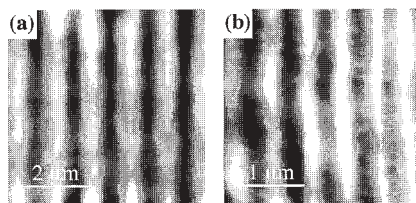


Figure 7. Birefringence SNOM images ( $\lambda = 690 \text{ nm}$ ) of optical gratings realized by SNOM on the 30/70 copolymer. The line spacing is (a) 1000 nm, and (b) 500 nm.<sup>[8,9]</sup>

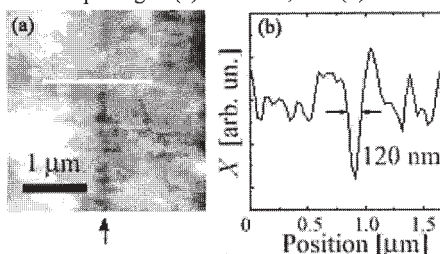


Figure 8. (a) Birefringence SNOM image of a line produced by previous writing with the SNOM probe at the arrow position. (b) Line profile at the horizontal stroke in (a).<sup>[8,9]</sup>

A laser diode ( $\lambda = 690 \text{ nm}$ ) was used to implement a polarization-modulation SNOM,<sup>[8]</sup> and optical patterns previously written by tracing vertical lines with the SNOM sensor (100 nm aperture) coupled with 488 nm light at fixed polarization were obtained with a writing speed of  $1 \mu\text{m/s}$  (Figure 7). Moreover, narrow vertical lines were produced at a speed of 30 nm/s (Figure 8a). The line profile of Figure 8(b) shows a purely optical writing/read-back resolution of the order of 100 nm. Blue light, by inducing *trans-cis-trans* cycles, caused

mainly optical orientation with negligible topography embossing. Local erasure of the information was also demonstrated by using writing light with rotating polarization.<sup>[8,9]</sup>

## Conclusion

An overview on the physical parameters relevant to optical data storage in PMA4 azobenzene polymers is presented. ESR line-shape analysis permits both to single out a suitable thermal procedure to obtain homogeneous substrates convenient for optical writing and to understand the significance of conformational rearrangements. We show that bit stability and working temperature range above the  $T_g$  can be modulated either by molar mass and molar mass distribution in homopolymers or by designing an adequate copolymer composition. Optical investigations, carried on millimeter and micrometer length scales, confirm the ESR findings. SNOM measurements proved the suitability of the adopted thermal procedure in order to obtain homogeneous substrates at the nanometer length scale.

## Acknowledgment

The authors thank the Italian MIUR and INFN (*CIPE project P5BW5*).

- [1] See for example, [1a] O. Tsutsumi, T. Shiono, T. Ikeda, G. Galli, *J. Phys. Chem. B* **1997**, *101*, 1332; [1b] J. G. Meier, R. Ruhmann, J. Stumpe, *Macromolecules* **2000**, *33*, 843; [1c] D. Bublitz, M. Helgert, B. Fleck, L. Wenke, S. Hvilsted, P. S. Ramanujam, *Appl. Phys. B* **2000**, *70*, 803.
- [2] L. Andreozzi, P. Camorani, M. Faetti, D. Palazzuoli, *Mol. Cryst. Liq. Cryst.* **2002**, *375*, 129.
- [3] L. Andreozzi, M. Faetti, G. Galli, M. Giordano, D. Palazzuoli, *Macromolecules* **2001**, *34*, 7325.
- [4] L. Andreozzi, M. Faetti, M. Giordano, D. Palazzuoli, M. Laus, G. Galli, *Macromol. Chem. Phys.* **2002**, *203*, 1636.
- [5] L. Andreozzi, M. Faetti, M. Giordano, D. Palazzuoli, M. Laus, G. Galli, *Mol. Cryst. Liq. Cryst.* **2003**, *398*, 97.
- [6] L. Andreozzi, M. Faetti, D. Palazzuoli, G. Galli, M. Giordano, *Mol. Cryst. Liq. Cryst.* in press.
- [7] S. Patané, A. Arena, M. Allegrini, L. Andreozzi, M. Faetti, M. Giordano, *Opt. Commun.* **2002**, *210*, 37.
- [8] M. Labardi, N. Coppedè, L. Pardi, M. Allegrini, M. Giordano, S. Patané, A. Arena, E. Cefali, *Mol. Cryst. Liq. Cryst.* **2003**, *398*, 33.
- [9] V. Likodimos, M. Labardi, L. Pardi, M. Allegrini, M. Giordano, A. Arena, S. Patané, *Appl. Phys. Lett.* **2002**, *82*, 3313.
- [10] [10a] E. Donth, *J. Polym. Sci. B, Polym. Phys.* **1996**, *34*, 2881; [10b] A. L. Kholodenko, T. A. Vilgis, *Phys. Rep.* **1998**, *298*, 251.
- [11] A. S. Angeloni, D. Caretti, M. Laus, E. Chiellini, G. Galli, *J. Polym. Sci., Polym. Chem. Ed.* **1991**, *29*, 1865.
- [12] M. Giordano, P. Grigolini, D. Leporini, P. Marin, *Phys. Rev. A* **1983**, *28*, 2474.
- [13] S. G. Carr, S. K. Kao, G. R. Luckhurst, C. Zannoni, *Mol. Cryst. Liq. Cryst.* **1976**, *35*, 7.
- [14] A. Abragam, B. Bleaney, "Electron Paramagnetic Resonance of Transition Ions", Clarendon Press, Oxford 1970.
- [15] L. Andreozzi, M. Giordano, D. Leporini, *Appl. Magn. Res.* **1993**, *4*, 279.
- [16] L. Andreozzi, M. Giordano, M. Faetti, D. Palazzuoli, *Appl. Magn. Res.* **2002**, *22*, 71.
- [17] [17a] P. Camorani, M. Labardi, M. Allegrini, *Mol. Cryst. Liq. Cryst.* **2001**, *372*, 365; [17b] L. Ramoino, M. Labardi, N. Maghelli, L. Pardi, M. Allegrini, S. Patané, *Rev. Sci. Instrum.* **2002**, *73*, 2051.